Study on Lubrication Performance of Journal Bearing with Multiple Texture Distributions

Jun Wang [1,2], Junhong Zhang [1,2], Jiewei Lin [1,*] and Liang Ma [1,3,*]

[1]   State Key Laboratory of Engine, Tianjin University, Tianjin 300072, China; wjun@tju.edu.cn (J.W.);
     zhangjh@tju.edu.cn (J.Z.)
[2]   Renai College, Tianjin University, Tianjin 301636, China
[3]   College of Aeronautical Engineering, Civil Aviation University of China, Tianjin 300300, China
[*]   Correspondence: linjiewei@tju.edu.cn (J.L.); mliang@tju.edu.cn (L.M.); Tel.: +86-137-5235-6026 (J.L.);
     +86-186-2261-5726 (L.M.)

Abstract: The lubrication performance of journal bearings with different sorts of uniformly distributed micro-spherical textures are studied in this paper. Geometries and dynamic models of journal bearings with pure concave/convex textures are developed. The validity of the proposed models is verified against the oil film pressure distribution from the literature. The effects of geometry parameters (the texture depth and the area density) on the load capacity and the friction coefficient of the bearing are analyzed and discussed. Results indicate that: the bearing load capacity is reduced by the concave spherical texture, but enhanced by the convex texture; both the concave and convex textures have a very slight influence on the friction coefficient. Aiming to further improve the bearing lubrication performance, a novel concave-convex composite texture is proposed and modelled. Results show that the composite texture can significantly improve both the load capacity and the friction coefficient, because the concave spherical segments among the convex ones protect the oil film from rupture near the main load region. The oil film region is expanded by the composite texture as well.

Keywords: micro-spherical texture; concave texture; convex texture; journal bearing; load capacity; friction coefficient; oil film

1. Introduction

Surface texture refers to the micro-concave/convex morphology. An appropriate surface texture can effectively reduce the wear of the friction pair and improve the load capacity of the oil film [1–4].

Hamilton et al. [5] proposed a liquid lubrication theory applicable to parallel surfaces and explained the lubrication mechanism based on surface micro-irregularities. This theory is in reasonable qualitative agreement with experimental results. Since then, the usage of the texture of technology to improve lubrication performance has aroused great interest among researchers. Etsion [6] found that micro-dimples on the friction surface were able to significantly improve the load capacity, the wear resistance and the friction coefficient compared with the non-textured components. This beneficial effect was verified experimentally using the Laser Surface Texturing (LST) technique.

The effects of different texture shapes and distributions on the lubrication characteristics of bearing have also been investigated. Cupillard [7] studied the effect of the dimple distribution and position on the dynamic lubrication characteristics of bearings using the computational fluid dynamics (CFD) method. It was found that the optimal distribution of dimples on the bearing surface depends on the operating conditions. When the eccentricity changes, the optimal location of the deep dimple changes accordingly. Brizmer [8] studied the effect of distribution and size of spherical texture on the load capacity of a sliding bearing. The optimum parameters of the dimples and the favorable LST mode for achieving maximum load capacity were found. Tala-Ighil et al. [9] studied the hydrodynamic

effect of a few deterministic texture shapes of a journal bearing, and found that the parallelepiped texture shows advantages in enhancing the bearing performance compared with other geometries. Based on the Reynolds equation, Rahmani et al. [10] used the genetic algorithm to study the effect of the cross-section shape of concave/convex textures on the lubrication performance of an infinitely wide journal bearing. The results showed that the convex texture was better than the concave texture at minimizing the friction factor and simultaneously maximizing the bearing capacity.

Increasing attention has been given to partial textures, which is an effective approach to improving bearing performance. Brizmer et al. [11] presented a partial texture that was able to significantly increase the load capacity. Rao et al. [12] developed a theoretical model of a partially textured slip slider and coupled stress fluid lubricated journal bearing. It was found that the partially textured slip was able to effectively improve the load capacity and reduce the friction coefficient.

From this literature review, it can be concluded that the concave/convex surface texture has attracted a lot of attention in the last two decades, and can serve as a micro hydrodynamic bearing to provide additional load capacity. The effects of texture shape, texture size, and texture distribution on load capacity have been systematically studied. Thus, the concave/convex surface texture seems to be a good candidate to improve the load capacity of bearing. However, apart from that, the friction coefficient is another important factor affecting the lubrication performance of bearing. However, the effect of concave or convex textures on the friction coefficient is not very significant, and is sometimes not even beneficial [13,14]. In 2011, Adatepe [13] conducted numerous experiments to investigate the performances of plain and micro-grooved journal bearings, in which the micro-grooves were made by cutting micro-channels around and across the journal bearing surfaces. The results showed that the friction coefficients of the journal bearings with micro-grooved textures were higher than those without texture. Furthermore, Adatepe [14] used various numerical methods to study the performances of plain, circumferential micro-grooved, herringbone micro-grooved, and transversally micro-grooved bearings. The bearings were then ranked in descending order by friction coefficients as follows: the transversally micro-grooved bearing, the herringbone bearing, the circumferential bearing and the plain bearing.

In this paper, mathematical models are developed to estimate the lubrication performance of journal bearings with surface textures. After validating the dynamic model, the effects of concave and convex spherical textures on the bearing lubrication performance are studied. On this basis, a novel concave-convex composite texture is further presented to improve the load capacity and the friction coefficient at the same time. Then, the effects of the composite texture characteristics on the lubrication performances are analyzed.

2. Simulation Model

2.1. Geometry of the Journal Bearing

Figure 1 shows the schematic of a journal bearing. The shaft rotates inside the bearing with a constant angular velocity ω. Points O_1 and O_2 correspond to the centers of the bearing and the shaft. The radii of the bearing and the shaft are R and r, respectively. ψ is the angle between the load direction and the centerline O_1O_2, and e is the eccentricity. The radial clearance is $c = R - r$ and the eccentric ratio is $\varepsilon = e/c$.

Assuming the radial clearance c of the journal bearing is much smaller than its radius ($c/R \sim 10-3$), the local clearance distribution for an untextured bearing can be approximated as [15]:

$$h_0 = c(1 + \varepsilon \cos \psi), \tag{1}$$
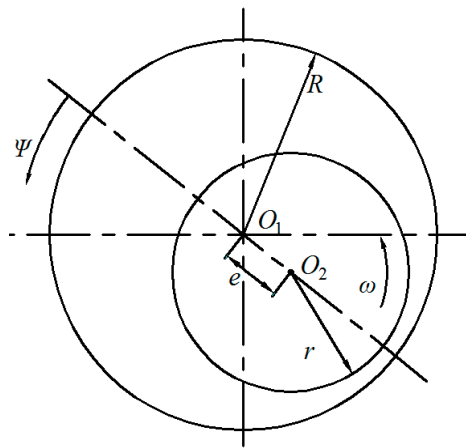
Figure 1. Schematic of the journal bearing.

2.2. Journal Bearing Model with Spherical Texture

Figure 2a shows the meshing scheme of the journal bearing, which is spread out in the circumferential direction. The bearing is uniformly meshed an M times N grid along the circumferential and the axial directions, respectively. Furthermore, every texture is simulated by spherical segments consisting of 10 squares along the x and z directions, as seen in Figure 2b. Every texture is simulated by a spherical segment consisting of the base radius r_b and the texture depth h_p located in the center of an imaginary rectangular grid. h_0 is the oil film thickness without texture and (x_0, z_0) are the coordinates of the texture center.

For a journal bearing with spherical texture, Equation (1) can be updated as follows:

$$h = h_0 \pm y, \tag{2}$$

The right side of the equation takes a positive sign when the spherical texture is convex and takes a negative sign when the spherical texture is concave. y is the coordinate of the bearing in the radial direction (see Figure 2b):

$$y = \sqrt{\left(\frac{h_p^2 + r_p^2}{2h_p}\right)^2 - (x - x_0)^2 - (z - z_0)^2} - \frac{h_p^2 + r_p^2}{2h_p}, \tag{3}$$
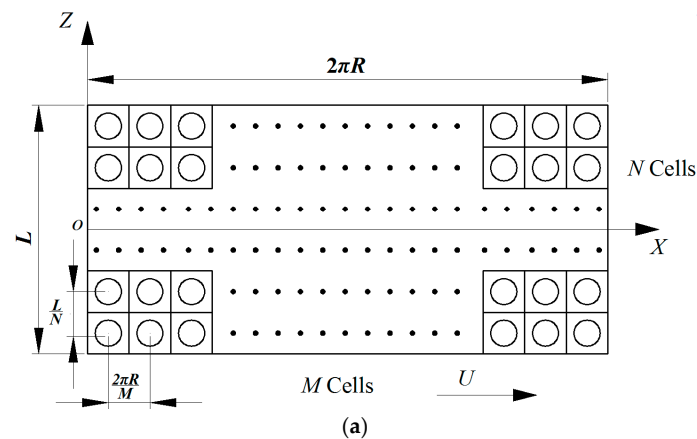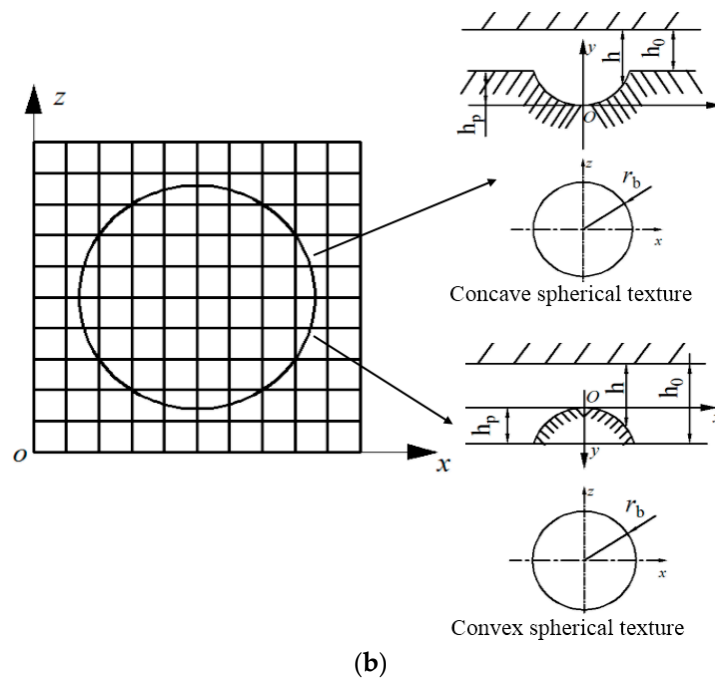

(a)

Figure 2. *Cont.*

(**b**)

Figure 2. Journal bearing model with spherical texture: (**a**) schematic of the bearing model and (**b**) grid details of different textures.

2.3. Numerical Solution

For a journal bearing under stable working conditions, the two-dimensional Reynolds equation can be expressed in the following form [16]:

$$\frac{\partial}{\partial X}\left(\frac{h^3}{\eta}\frac{\partial p}{\partial X}\right) + \frac{\partial}{\partial Z}\left(\frac{h^3}{\eta}\frac{\partial p}{\partial Z}\right) = 6U\frac{\partial h}{\partial X}, \tag{4}$$

where p is the oil film pressure at a specific point on the bearing surface, U is the linear sliding velocity of the shaft relative to the bearing and η is the dynamic viscosity of the lubricant.

- Solution of the Reynolds equation

  (a)　The Reynolds boundary is applied in the bearing modelling process. The effect of cavitation is not included in the analysis, either in terms of the single-phase analysis used or in the application of the boundary conditions, which is considered in a thermo-hydrodynamic analysis of the bearing with the CFD approach [17,18].

  (b)　In the *XOZ* plane, the journal bearing is meshed into m and n grids along the X and Z directions, where m is $10 \times M$ and n is $10 \times N$.

  (c)　The five-points difference method is used to discretize Equation (4). The symmetric successive over relaxation (SSOR) method is used to solve the discrete algebraic system of equations and the pressure p is obtained.

- Solution of lubrication parameters of the journal bearing

  (a)　Load capacity of the journal bearing

The calculated oil film pressure p is numerically integrated in the whole fluid domain along the X and Y directions, and the load capacities W_X and W_Y can be obtained as follows:

$$W_X = \int_{-\frac{L}{2}}^{\frac{L}{2}} \left(\int_0^{2\pi R} p \cos \psi dX \right) dZ$$
$$W_Y = \int_{-\frac{L}{2}}^{\frac{L}{2}} \left(\int_0^{2\pi R} p \sin \psi dX \right) dZ \quad , \tag{5}$$

In both cases, the total load capacity W and the attitude angle can be calculated as:

$$W = \sqrt{W_X{}^2 + W_Y{}^2}, \tag{6}$$

$$\psi = \frac{X}{R}, \tag{7}$$

(b)   Friction coefficient

The shear stress τ of the slip plane between the friction pairs can be given as [19]:

$$\tau = \frac{h}{2}\frac{\partial p}{\partial X} + \frac{\eta}{h}U, \tag{8}$$

The friction force F can be expressed as the integral of the shear stress on the slip plane:

$$F = \iint \left(\frac{h}{2}\frac{\partial p}{\partial X} + \frac{\eta}{h}U \right) dXdZ, \tag{9}$$

According to Equations (6) and (9), the expression of the friction coefficient μ can be given as:

$$\mu = \frac{F}{W}. \tag{10}$$

3. Model Verification

To verify the proposed model of the journal bearing with textures, the results from [20] are used. A group of dimensionless parameters characterizing the journal bearing are given as follows: the eccentricity ratio is 0.65, the width-radius ratio is 1, the dimensionless texture depth is 0.5, and the dimensionless spherical texture radius is 128. The grid amounts are $m = 600$ and $n = 200$. The distributions of the oil film pressure from the simulation of this study and from the literature are shown in Figure 3. It can be seen that the calculated oil film pressure agrees with the tested data well, which verifies the validity of the proposed method.
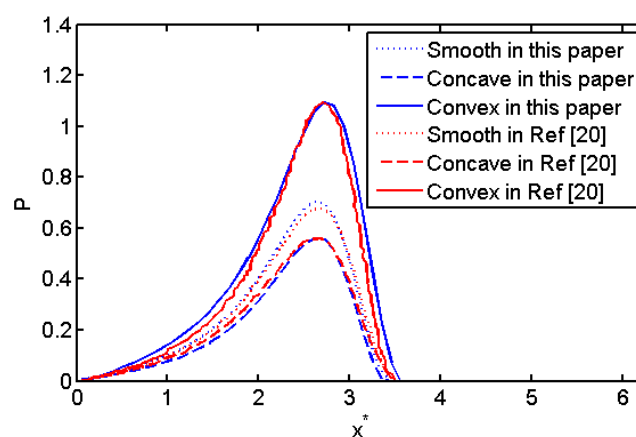

Figure 3. Comparison of circumferential film pressure distributions between proposed model and [20].

4. Lubrication of the Concave/Convex Textured Bearing

The numerical simulation in this study is initiated with the following parameters: (i) the radius of the journal bearing R is 0.035 m; (ii) the width of the journal bearing L is 0.0656 m; (iii) the radial clearance c is 5×10^{-5} m; (iv) the eccentric ratio ε is 0.65; (v) the linear sliding velocity of the shaft relative to the bearing U is 0.5 m/s; (vi) the dynamic viscosity of the lubricant η is 0.028 Pa·s; and (vii) a convergence study concerning the mesh size is investigated, the suitable numbers of grids m and n are 310 and 100, respectively. The texture is uniformly arranged on the inner wall of the bearing, and there are 31 spherical segments along the X direction and 10 spherical segments along the Z direction.

4.1. Effect of Texture Depth

With a fixed area density λ of 0.5, simulations with different texture depths h_p from 5×10^{-7} to 3×10^{-6} m are performed. The load capacity W and the friction coefficient μ of the plain bearing, the concave textured bearing, and the convex textured bearing are plotted in Figure 4. For $h_p = 5 \times 10^{-7}$m, the load capacity of the bearing with convex texture is the highest, that of the plain bearing is in the middle, and that of the concave textured bearing is the lowest. The load capacity of the bearing with convex spherical texture increases with increasing texture depth h_p from 5×10^{-7} m to 3×10^{-6} m, while that of the concave textured bearing decreases in the same case. Taking the load capacity of the plain bearing (1014 N) as the baseline value, when the texture depth h_p is increased to 3×10^{-6} m, the load capacity of the convex textured bearing (1171 N) greatly improves by 7.93%, while that of the concave textured bearing decreases by 6.54%. The friction coefficient, seen in Figure 4b, is not affected by the texture depth as much as the loading capacity. The friction coefficient of the convex textured bearing reduces with increasing area density, but the decrement is slight, and that of the concave textured bearing increases a little bit. The lowest friction coefficient of the convex textured bearing can be achieved (0.072) at $h_p = 3 \times 10^{-6}$ m, the improvement is only 0.96% comparing with the plain bearing (0.0727), and that of the concave (0.0728) gets even worse, but also to a trivial degree of 0.14%.
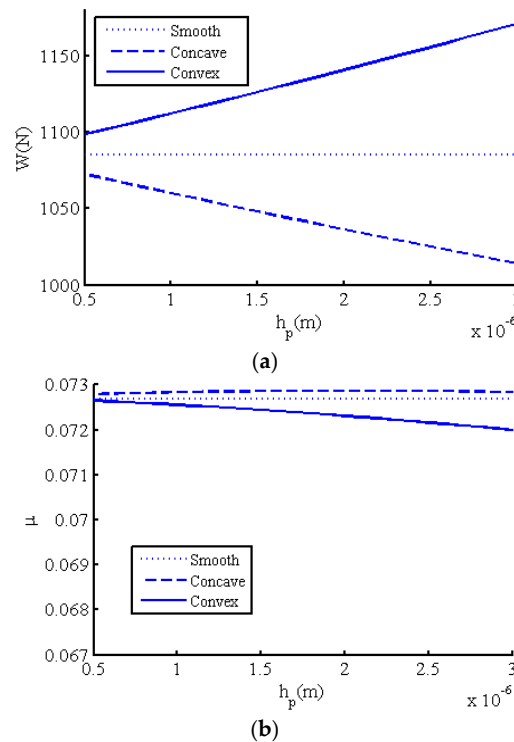

(a)

(b)

Figure 4. Effect of the texture depth on (**a**) the load capacity and (**b**) the friction coefficient.

4.2. Effect of Area Density

In the case of 2×10^{-6} m texture depth, simulations with different area densities λ from 0.03 to 0.8 are performed, and the load capacity W and the friction coefficient μ of the plain bearing, the concave textured bearing and the convex textured bearing are plotted in Figure 5. From Figure 5a, it can be observed that the load capacity of the bearing with convex spherical texture increases with increasing area density λ from 0.03 to 0.8, while that with the concave spherical texture decreases with the increase of area density in the same range. For $\lambda = 0.8$, the load capacity of the convex textured bearing is 1173 N, and the increment is 8.11%, relative to the plain bearing (1085 N). With the same area density, the load capacity of the concave textured bearing decreases to 1010 N by 6.91% relative to the plain bearing. From Figure 5b, it is shown that the friction coefficient of the concave textured bearing hardly changes with changing area density, and that of the convex textured bearing decreases with increasing area density, but the beneficial effect is very slight. For $\lambda = 0.8$, compared with the plain bearing, the friction coefficient of the concave textured bearing increases by 0.28% to 0.0729, and that of the convex textured bearing decreases by 0.96% to 0.072.
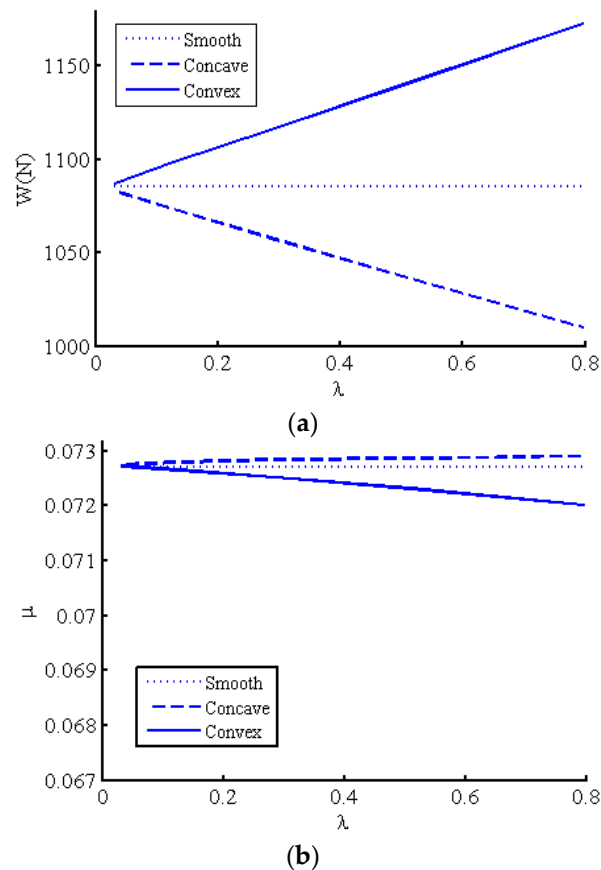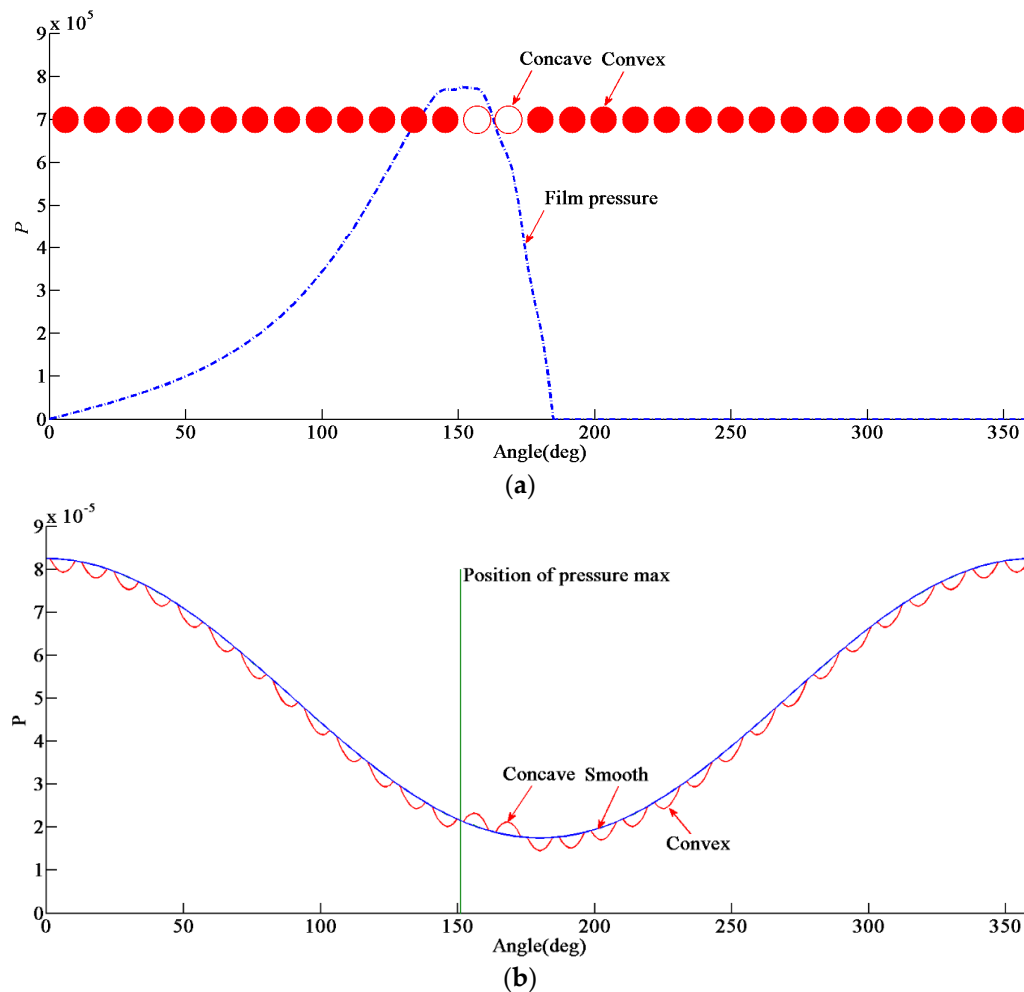

Figure 5. Effect of texture area density on (**a**) the load capacity and (**b**) the friction coefficient.

5. Concave-Convex Composite Spherical Texture

The relationships between texture parameters and lubrication performances of the journal bearing are found based on the above analysis. It is indicated that, with a pure texture form (pure convex or pure concave), the friction coefficient is hardly influenced, regardless of the parameter type and value. However, the friction coefficient is an important factor that should be reduced in the case of journal bearing lubrication. To this end, a concave-convex composite spherical texture is presented in this section. The composite texture distribution along the circumference direction is shown in Figure 6a, where the red solid dot indicates the convex texture and the hollow dot represents the concave texture.

Two rows of concave spherical segments are arranged near the main loading region and the convex spherical segments are used elsewhere. The blue dashed line in Figure 6a is the circumferential film pressure distribution. It can be seen that the film pressure reaches the peak at the boundary where the texture type alternates from convex to concave, and drops sharply near the region where the texture type changes back from concave to convex. Figure 6b is the circumferential film thickness distribution diagram, in which the red line above the blue line represents the film thickness at the position of the concave spherical segment, and that below the blue line represents the film thickness at the position of the convex spherical segment.

Figure 6. Distribution of concave-convex composite spherical texture: (**a**) circumferential film pressure distribution, (**b**) circumferential film thickness distribution diagram.
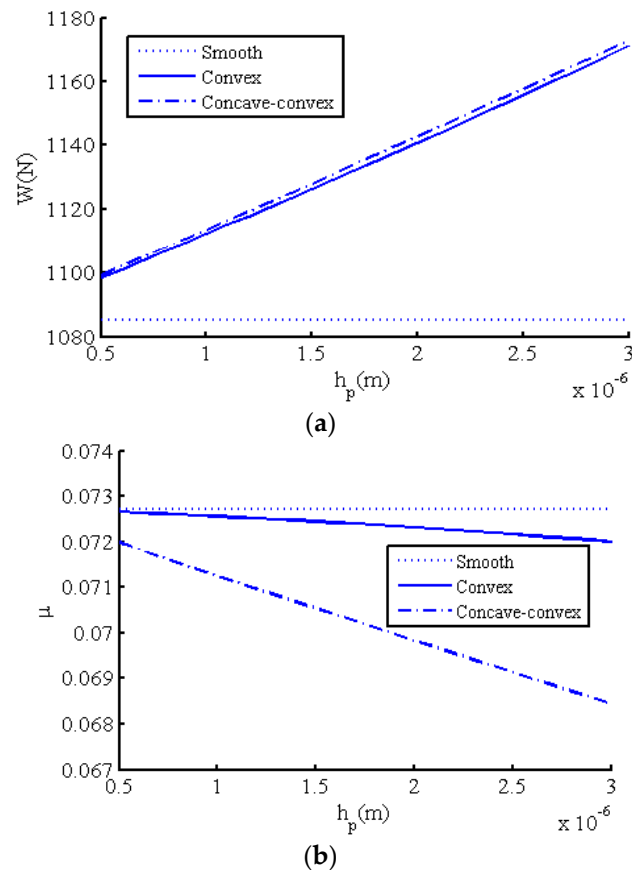
To discuss the lubrication performance of the composite texture, comparisons between the plain, the convex, and the composite textured bearings are carried out. The pure concave texture case is not considered, because its lubrication performance has already been found to be the worst.

5.1. Effect of Texture Depth

With a fixed area density λ of 0.5, simulations with different texture depths h_p from 5×10^{-7} to 3×10^{-6} m are performed. The load capacity W and the friction coefficient μ of the bearing with concave-convex composite spherical texture, convex spherical texture and no texture are plotted in Figure 7. It is found that the load capacities of the convex and the composite textured bearings both increase with increasing texture depth. The increment of the composite texture is slightly higher than

that of the convex texture. The load capacities of both sorts of textured bearing reach the maximum value at $h_p = 3 \times 10^{-6}$ m together. The load capacity of the composite textured bearing is greatly improved to 1173 N by 8.11% relative to that of the plain bearing (1085 N), and the improvement of the convex textured bearing is quite similar (7.9%).
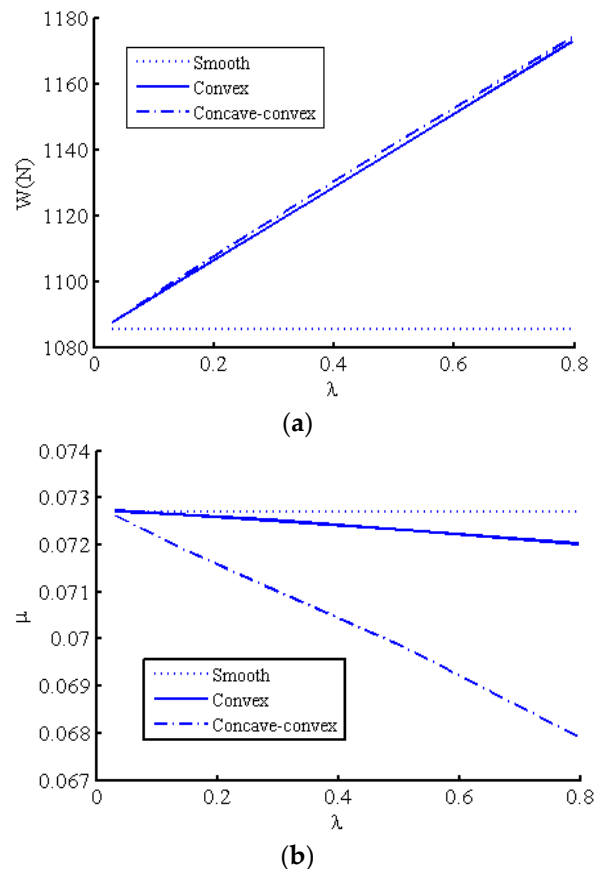
Figure 7. Effect of texture depth on (**a**) the load capacity and (**b**) the friction coefficient.

In the texture depth range considered, the initial friction coefficient (at $h_p = 5 \times 10^{-7}$ m) of the composite textured bearing is lower than those of plain bearing and the convex textured bearing. The friction coefficients of the bearings with the composite texture and the convex texture both decrease with increasing texture depth. However, Figure 7b clearly shows an obviously greater reduction in friction coefficient for the composite textured bearing than the convex one. Since both the friction coefficient trends are monotonous, the lowest values can be obtained at the greatest texture depth of 3×10^{-6} m. A significant reduction in the friction coefficient is achieved by the composite textured bearing from 0.072 (plain bearing) to 0.0684 by 5.91%, which can be regarded as a considerable beneficial effect in lubrication performance of the journal bearing.

5.2. Effect of Area Density

With a fixed texture depth h_p of 2×10^{-6} m, the load capacity W and the friction coefficient μ of different textured bearings are simulated under various of area densities λ from 0.03 to 0.8. From Figure 8, it can be observed that the area density λ of the composite textured not only has a great effect on the load capacity W, but also significantly affects the friction coefficient μ of the bearing. Both the pure convex and the convex-concave composite textures are able to enhance the bearing load capacity when the texture depth is increased. In addition, the improvements of both sorts of texture in the load capacity are nearly the same. For $\lambda = 0.8$, the load capacity of the composite textured bearing increases

by 8.2% from 1085 N (plain bearing) to 1174 N and that of the convex one increases to 1173 N as well. Compared with the pure texture (convex or concave), the composite texture has a significant effect on the friction coefficient. As seen in Figure 8b, the friction coefficients of the bearing with both texture types decrease with increasing area density. It should be noted that the decrement of the composite textured bearing caused by the increase of area density is much greater than that of the pure convex textured bearing. At $\lambda = 0.8$, the maximum reduction in friction coefficient of the composite bearing is 6.6%, based on the plain bearing. In the same case, the biggest decrement of the convex textured bearing is only 0.97%, which is far smaller than the composite textured bearing.

Figure 8. Effect of texture area density on (**a**) the load capacity and (**b**) the friction coefficient.

That is to say, the convex-concave composite texture has considerable potential for improving lubrication performance in terms of increasing load capacity and decreasing friction coefficient.

Based on the above studies, a combination of texture depth and area density is used for both the convex and the composite cases, which are $h_p = 3 \times 10^{-6}$ m and $\lambda = 0.8$. The oil film pressure distributions of the plain, the convex and the composite textured bearings are calculated and compared in Figure 9. Taking the plain bearing as a reference, the load capacity and the friction coefficient of the convex and the composite textured bearings are calculated with the optimal texture depth and area density and listed in Table 1. With the optimal texture parameters, both the pure convex and the composite textures can improve the lubrication performance of bearing. The improvements in load capacity are the same for both texture types. The reductions of the friction coefficient are significantly different between the two cases; the composite texture has a much greater reduction than the convex texture.

Figure 9 shows the circumferential oil film pressure distributions of the plain bearing, the convex textured bearing and the concave-convex composite textured bearing. The circumferential length with

oil film of the convex textured bearing is the same as that of the plain bearing. However, the oil film pressure in the convex texture in the main load region is much higher than that of the plain bearing. For the composite texture, the oil film is still higher than the plain bearing, but lower than the convex texture at peak, and higher than the convex texture at other locations. Additionally, the pressurized area of the composite textured bearing is wider than those of the plain and the convex textured bearings by 10 degrees. A wider pressurized area indicates a wider load region and a higher oil film pressure throughout the whole departure half of the contact area.
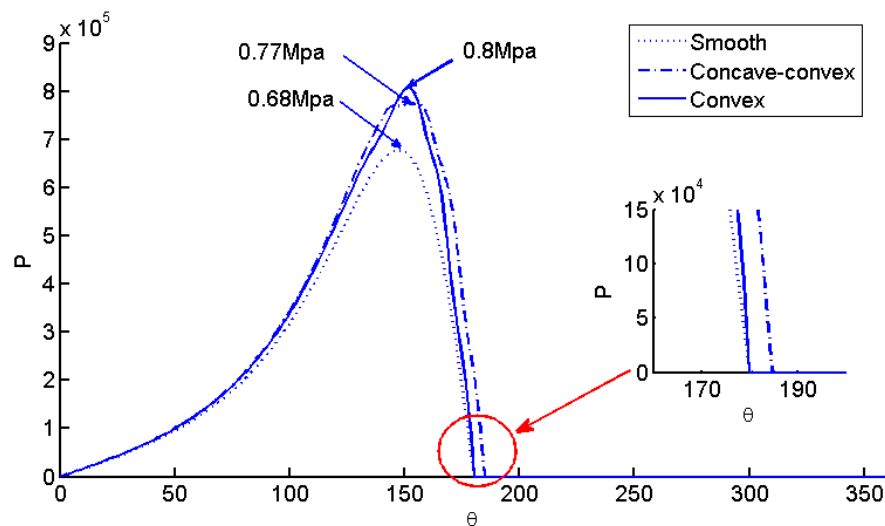

Figure 9. Circumferential oil film pressure distribution.

Table 1. Load capacity and friction coefficient of bearings with the optimal parameters.

Texture Types	W (KN)	ΔW (%)	μ	Δμ (%)
Plain (baseline)	1.09	0	0.073	0
Convex	1.22	+11.93	0.072	−1.4
Concave-convex composite	1.22	+11.93	0.066	−9.59

6. Conclusions

The potential use of the spherical texture is studied in terms of the effects of texture type and parameters on the bearing lubrication performance. A theoretical model of a textured bearing is developed and validated. A novel convex-concave composite texture is proposed after discussing the effects of texture depth and area density on the load capacity and the friction coefficient of the bearing. The performance of the composite texture is then simulated and compared with the convex texture. The main conclusions can be drawn as follows:

(1) The load capacity of the concave spherical textured bearing is lower than that of the plain bearing, and the friction coefficient is hardly affected by the concave texture. The convex spherical texture can increase the bearing load capacity and friction coefficient at the same time, but the reduction in friction coefficient is fairly slight.

(2) The concave-convex composite spherical texture can improve the load capacity and the friction coefficient of the bearing. In contrast to the convex texture, the beneficial effect introduced by the composite texture on the friction coefficient is as significant as that on load capacity.

(3) In addition to the load capacity and the friction coefficient, the oil film region is expanded in the composite texture case, as well. That is to say, the proposed convex-concave composite texture has significant potential for lubrication improvement of the bearing.

Author Contributions: Jun Wang developed the bearing models with textures and conducted the analyses; Junhong Zhang contributed analysis tools; Jiewei Lin wrote and revised the paper; Liang Ma developed the baseline bearing model.

Conflicts of Interest: The authors declare no conflict of interest.

Nomenclature

Parameters and Variables

c	radial clearance
e	eccentricity
F	friction force
h	film thickness
h_0	film thickness of the untextured bearing
h_p	texture depth
L	width of the journal bearing
m, n	number of grid points along X and Z directions
M, N	number of meshes along X and Z directions
O_1, O_2	centers of the journal bearing and the shaft
p	film pressure
R, r	radii of the journal bearing and the shaft
r_b	base radius of the spherical texture
U	relative linear sliding velocity of the bearing and the shaft
W	total load capacity
W_X, W_Y	load capacities along X and Y direction
x, y, z	local coordinates of the mesh along X, Y and Z directions
X, Y, Z	coordinates of the bearing along circumferential, radial and axial directions
(x_0, z_0)	coordinates of the texture center
ΔW	ratio of the load capacity between the textured bearing and the smooth bearing
$\Delta \mu$	ratio of the friction coefficient between the textured bearing and the smooth bearing
ε	eccentric ratio
η	dynamic viscosity of lubricant
μ	friction coefficient
τ	shear stress of the slip plane between the friction pairs
ψ	angle between the load coordinate and the centerline O_1O_2
ω	angular velocity of the shaft

References

1. Gualtieri, E.; Borghi, A.; Calabri, L.; Pugno, N.; Valeri, S. Increasing nanohardness and reducing friction of nitride steel by laser surface texturing. *Tribol. Int.* **2009**, *42*, 699–705.
2. Andersson, P.; Koskinen, J.; Varjus, S.; Gerbig, Y.; Haefke, H.; Georgiou, S.; Zhmud, B.; Buss, W. Microlubrication effect by laser-textured steel surfaces. *Wear* **2007**, *262*, 369–379.
3. Etsion, I. State of the art in laser surface texturing. *Trans. ASME* **2005**, *127*, 248–253. [CrossRef]
4. Erdemir, A. Review of engineered tribological interfaces for improved boundary lubrication. *Tribol. Int.* **2005**, *38*, 249–256. [CrossRef]
5. Hamilton, D.B.; Walowit, J.A.; Allen, C.M. A theory of lubrication by microirregularities. *J. Basic Eng.* **1966**, *88*, 177–185. [CrossRef]
6. Etsion, I. Improving tribological performance of mechanical components by laser surface texturing. *Tribol. Lett.* **2004**, *17*, 733–737. [CrossRef]
7. Cupillard, S. Lubrication of Conformal Contacts with Surface Texturing. Licentiate Thesis, Lulea Tekniska University, Luleå, Sweden, 2007.
8. Brizmer, V.; Kligerman, Y. A laser surface textured journal bearing. *J. Tribol.* **2012**, *134*, 1–9. [CrossRef]

9. Tala-Ighil, N.; Maspeyrot, P.; Fillon, M.; Abdelhamid, B. Hydrody-namic effects of texture geometries on journal bearing surfaces. In Proceedings of the The 10th International Conference on Tri-bology, Bucharest, Romania, 8–10 November 2007; pp. 47–52.

10. Rahmani, R.; Mirzaee, I.; Shirvani, A.; Shirvani, H. An analytical approach for analysis and optimisation of slider bearings with infinite width parallel textures. *Tribol. Int.* **2010**, *43*, 1551–1565. [CrossRef]

11. Brizmer, V.; Kligerman, Y.; Etsion, I. A laser surface textured parallel thrust bearing. *Tribol. Trans.* **2003**, *46*, 397–403. [CrossRef]

12. Rao, T.V.V.L.N.; Rani, A.M.A.; Nagarajan, T.; Hashim, F.M. Analysis of couple stress fluid lubricated partially textured slip slider and journal bearing using narrow groove theory. *Tribol. Int.* **2014**, *69*, 1–9. [CrossRef]

13. Adatepe, H.; Bıyıklıoglu, A.; Sofuoglu, H. An experimental investigation on frictional behavior of statically loaded micro-grooved journal bearing. *Tribol. Int.* **2011**, *44*, 1942–1948. [CrossRef]

14. Adatepe, H.; Bıyıklıoglu, A.; Sofuoglu, H. An investigation of tribological behaviors of dynamically loaded non-grooved and micro-grooved journal bearings. *Tribol. Int.* **2013**, *58*, 12–19. [CrossRef]

15. Pinkus, O.; Sternlicht, B. *Theory of Hydrodynamic Lubrication*; McGraw-Hill: New York, NY, USA, 1961.

16. Tala-Ighil, N.; Maspeyrot, P.; Fillon, M.; Bounif, A. Effects of surface texture on journal-bearing characteristics under steady-state operating conditions. *Proc. IMechE Part J J. Eng. Tribol.* **2007**, *221*, 623–633. [CrossRef]

17. Tucker, P.G.; Keogh, P.S. A generalized computational fluid dynamics approach for journal bearing performance prediction. *Proc. IMechE Part J J. Eng. Tribol.* **1995**, *209*, 99–108. [CrossRef]

18. Shahmohamadi, H.; Rahmani, R.; Rahnejat, H.; Garner, C.P.; Dowson, D. Big end bearing losses with thermal cavitation flow under cylinder deactivation. *Tribol. Lett.* **2015**, *57*. [CrossRef]

19. Rao, T.V.V.L.N.; Rani, A.M.A.; Nagarajan, T.; Hashim, E.M. Analysis of slider and journal bearing using partially textured slip surface. *Tribol. Int.* **2012**, *56*, 121–128. [CrossRef]

20. Jiang, Y.; Ma, F.; Liu, P.; An, Q. School of Mechanical and Power Engineering, East China University of Science and Technology. Effects of micro-shperical surface texture on the performance of journal bearings. *J. East China Univ. Sci. Technol.* **2014**, *40*, 539–544. (In Chinese)